group. Finally, the presence of a singlet broad band at 7.01 ppm is due to the faraway of nitrogen atom of $–NH_2$ from complexation, Fig. 4.

Table 2. IR frequencies (cm^{-1}) of $[Se(AA)_2Cl_2]$ complexes

Compound	ν(O-H) ν(N-H)	ν(COO⁻)		δ(NH_2)	ν(M-O)	ν(M-N)
		Asym	Sym			
I	3163	1667	1403	--	524	466
II	3136	1621	1403	--	520	470
III	3180	1593	1402	--	497	428
IV	3124	1617	1409	--	523	439
V	3027	1622	1407	1487	540	455

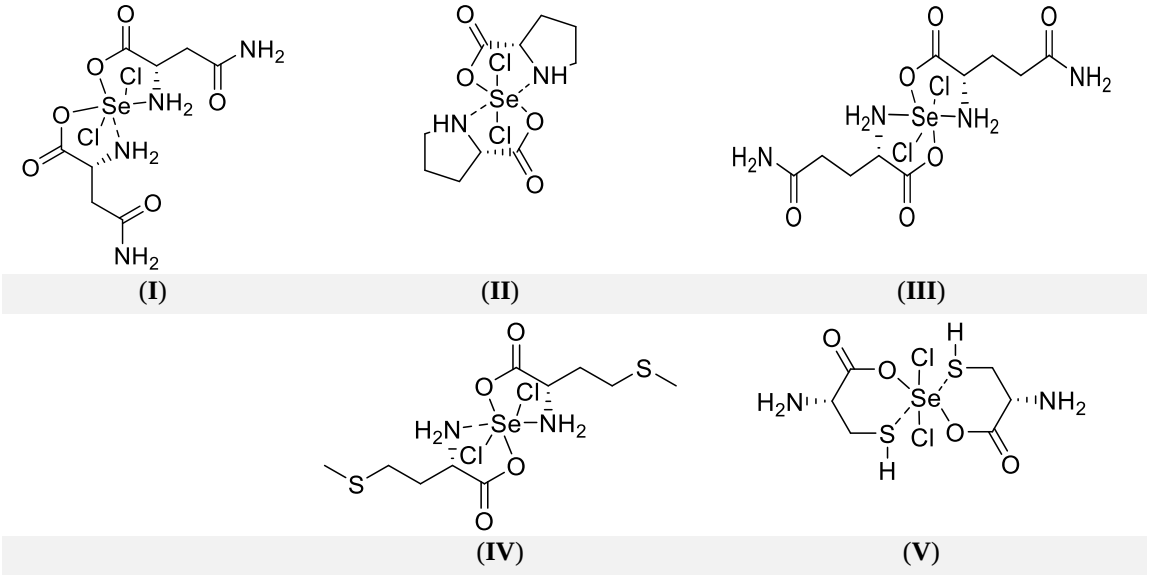

Fig. 4. Speculated structures of $[Se(AA)_2Cl_2]$ complexes (AA= *Asp*, *Pro*, *Glu*, *Met* and *Cys*).

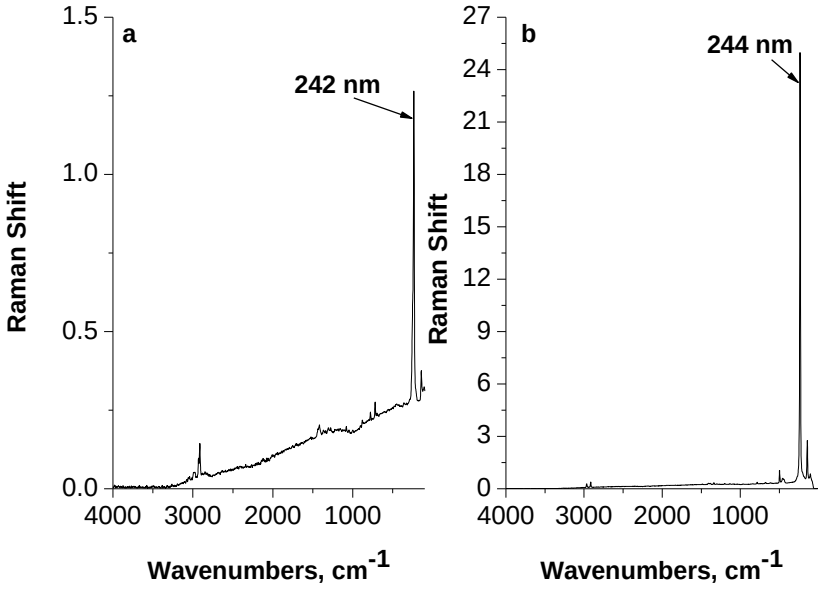

Fig. 5. Raman laser spectrum of a- Se-*Met* and b- Se-*Cys* complexes

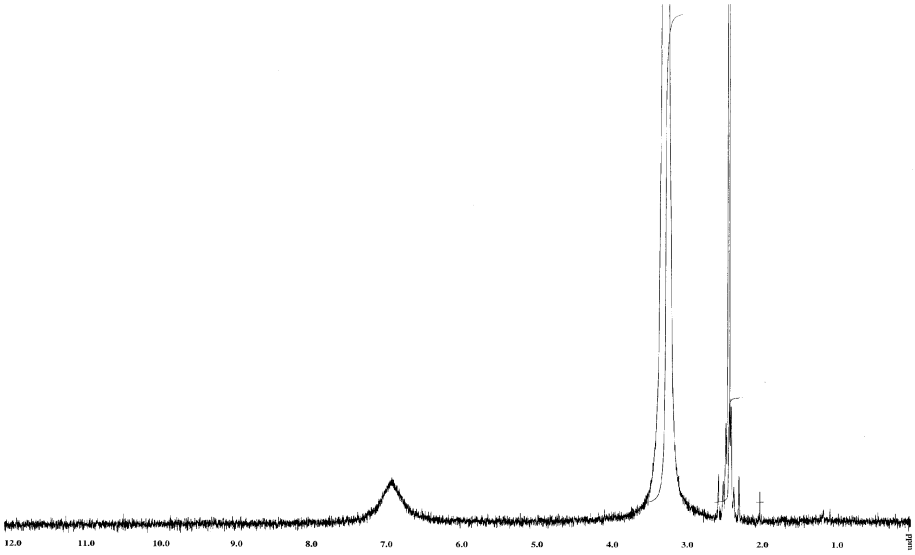

Fig. 6. ^{1}H-NMR spectrum of the Se-*Cys* complex.

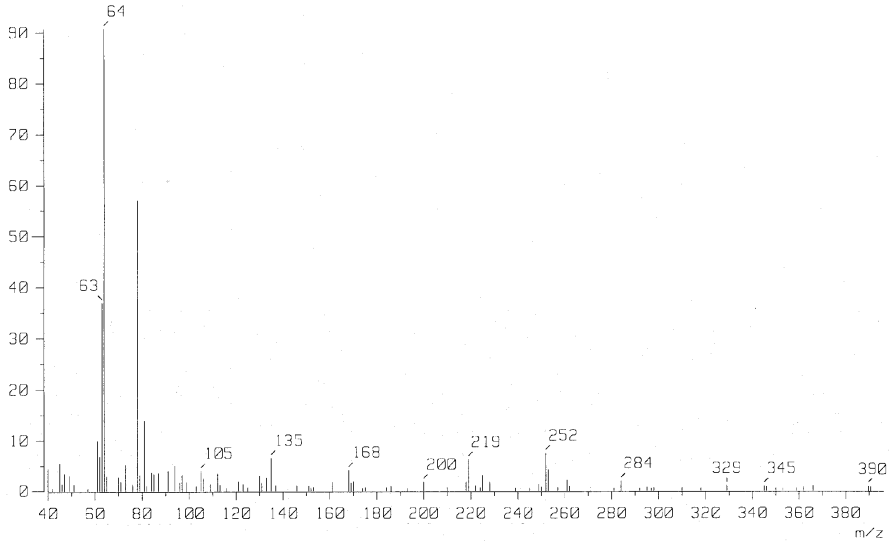

Fig. 7. Mass spectrum of Se-*Cys* complex.

Mass Spectra

*Chemical shifts of the Se-Cys (**V**) complex:* The mass spectral data of the [Se(*Cys*)$_2$(Cl)$_2$] complex are presented in Fig. 7. The mass spectrum of Se-*Cys* complex showed a molecular ion peak that is in a good agreement with the expected value. The mass spectrum of Se-*Cys* shows a peak at 390 m/z, which was assigned as a [M] peak. The *Cys* molecule was thought to produce ions at m/z 345, 329, 284,252, 219,200, 168, 135, 105, 64, and 63, respectively. The m/z 78 ion, which is a Se-*Cys* (**V**) complex, is containing one selenium atom.

XRD Spectra

The X-ray diffraction patterns of the [Se(*Cys*)$_2$(Cl)$_2$] complex with selenium nanoparticles are shown in Fig. 8. The diffraction peaks present at 2θ (degrees) of 23.42°, 29.57°, 42.05°, 43.75°, 45.47°, 51.43°, 55.70°, 61.46°, 65.09° and 71.59° correspond to (100), (101), (110), (102), (111), (201), (112), (202), (210) and (113) planes of selenium, respectively. The diffraction peaks within the 2θ region due to hexagonal crystal structure of selenium are in agreement with the standard data (JCPDS card No. 01-071-4647), as shown in Fig. 9. The particle size of selenium was estimated using Scherrer's eq. [36]

$$D = \frac{0.89\lambda}{\beta \mathrm{Cos}\theta} \quad (1)$$

where D = grain size, K = constant equal to 0.94, λ = wavelength of the X-ray radiation, β = full width at half maximum and θ = diffraction angle. The particle size of selenium nanoparticles is found to

be ~ 10 nm. The diffraction pattern due to (100), (101), (110), (102), (111) and (201) directions of hexagonal phase of selenium is shown in Fig. 9. The d-spacing values for the diffraction pattern match well with the hexagonal selenium.

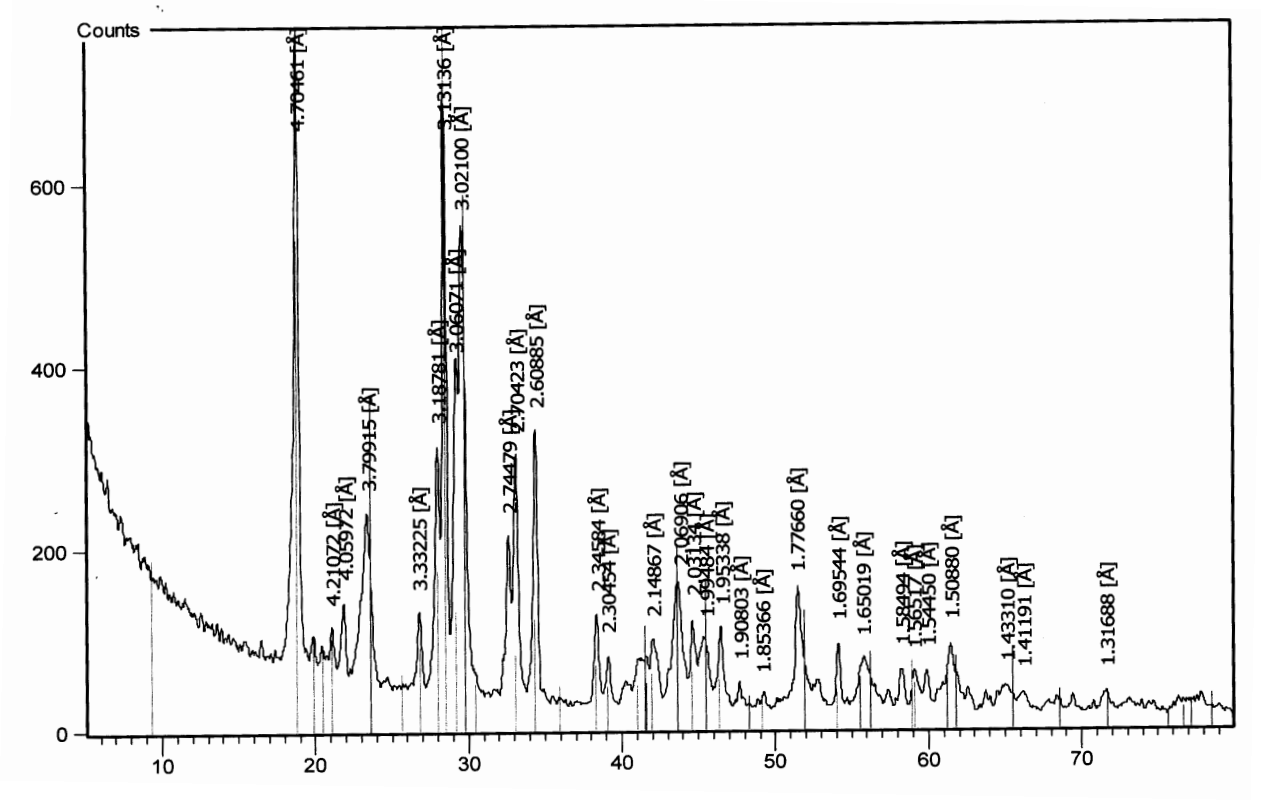

Fig. 8. XRD spectrum of Se-*Cys* complex.

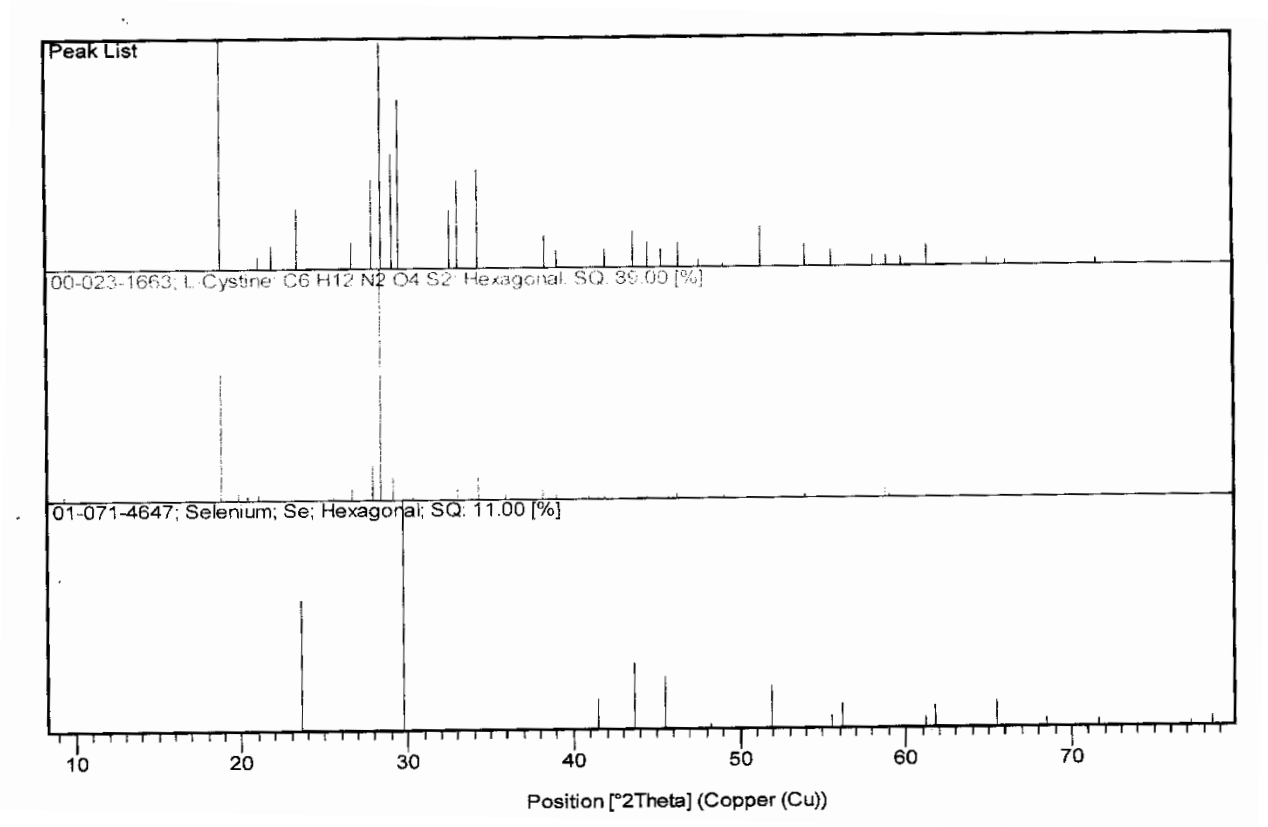

Fig. 9. Standard XRD spectrum of *Cys* and Se-*Cys* complex with selenium hexagonal structure.

SEM, TEM and EDX Spectra

The scanning electron microscope (SEM) image of the $[Se(Cys)_2(Cl)_2]$ complex with selenium nanorods and hexagonal structure is illustrated in Fig. 10. The SEM image reveals that the selenium nanorods are of uniform size with a mean diameter of ~ 10 nm. It can be seen that nanorods are of several micrometers in length with diameter ranging from 10 μm. Energy dispersive X-ray analysis (EDX) was used to identify and determine the chemical composition of the Se-*Cys* complex. EDX pattern of the Se-*Cys* complex is shown in Fig. 11. Weak signals concerning O atoms have been recorded along with the strong peak due to Se atom. EDX analysis indicates the presence of O, S, C, and Cl with very low intensity, so this analysis supported the purity of the selenium particles.

The transmission electron microscopy images were performed using JEOL 100s microscope. Fig. 12 shows the transmission electron microscope (TEM) image of Se-*Cys* complex selenium nanorods. The image shows that the nanorods are with an average diameter of ~ 10 nm.

.

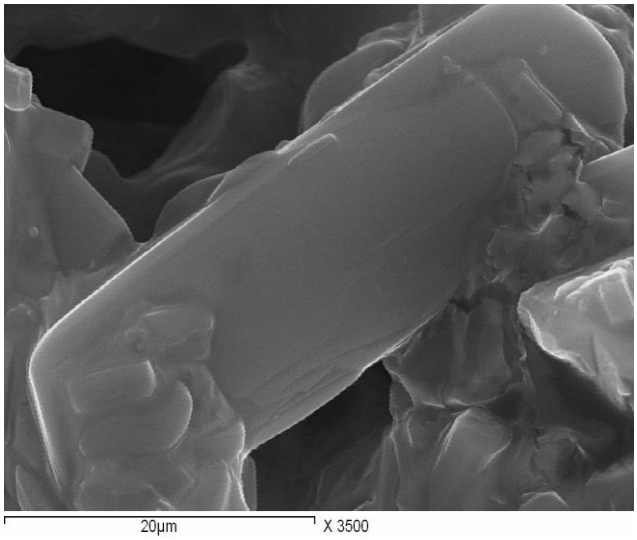

Fig. 10: SEM image of Se-*Cys* complex.

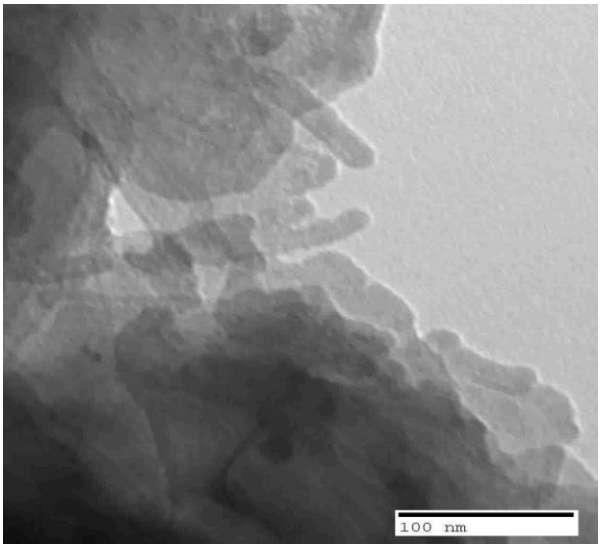

Fig. 12. TEM image of Se-*Cys* complex

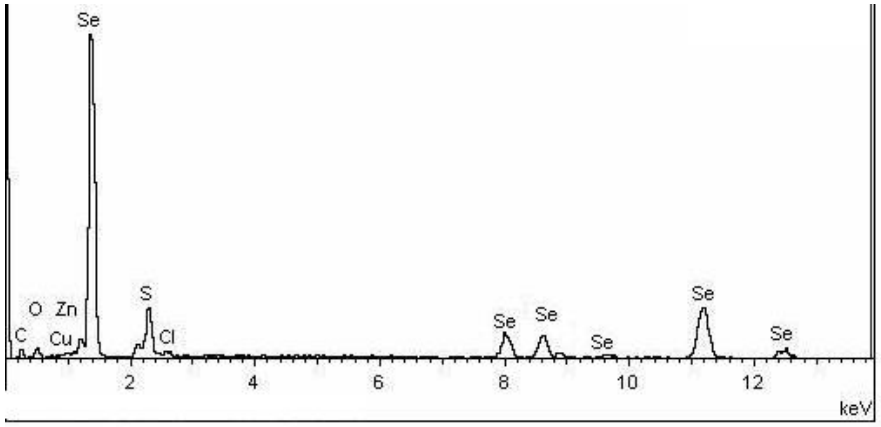

Fig. 11. EDX spectrum of Se-*Cys* complex.

Thermal analysis

Thermal stability of $[Se(AA)_2Cl_2]$ complexes (AA= *Asn*, *Pro*, *Gln*, *Met* and *Cys*) complexes was checked based on thermo gravimetric and its differential analyses started from room temperature till 800 ^oC under N_2 atmosphere. The TG curves were redrawn as mg mass loss *versus* temperature. The thermal decomposition curves (TG) are given in Fig. 13.

Asn-Se complex: Thermal decomposition of *Asn*-Se complex (**I**) occurs in four steps. The 1st degradation step takes place in the temperature range of 179-222 ^oC at DTG_{max} = 196 ^oC (endo) and it correspond to a mass loss of 15.043%. The 2nd step occur within the temperature range of 296-367 ^oC at DTG_{max} = 317 ^oC (endo) which was assigned to the decomposition of *Asn* molecule with a weight loss of 52.949%. The 3rd step occurs within the temperature range of 433-475 ^oC at DTG_{max} = 452

°C which is due to loss of organic moiety with a weight loss of 8.835%. The last decomposition step takes place within the temperature range of 573-663 °C with mass loss of 21.464%. The residual carbon atoms (1.709%) in the final product remain stable till 800 °C.

Pro-Se complex: The thermal decomposition of *Pro*-Se complex (**II**) occurs in three steps. The first degradation step takes place in the temperature range of 121-167 °C at DTG_{max} = 136 °C (endo) and it corresponds to the loss of one chlorine atom with mass loss of 7.697%. The second step occurs within the temperature range of 275-383 °C at DTG_{max} = 325 °C (endo) which was assigned to the decomposition of two *Pro* and one chlorine molecule with weight loss of 75.077%. The third step occurs within the temperature range of 527-625 °C at DTG_{max} = 563 °C (endo) which was assigned to the loss of organic moiety with a weight loss of 12.420%. The few carbon atoms in the final product remain stable till 800 °C with mass loss of 4.806%.

Gln-Se complex: The thermal decomposition of *Gln*-Se complex (**III**) occurs in four successive steps. The first degradation step takes place in the temperature range of 46-55 °C at DTG_{max} = 44 °C and it corresponds to the loss of water molecules with a weight loss of 2.183%. The second step occurs within the temperature range of 156-202 °C at DTG_{max} = 172 °C (endo) which was assigned to the loss of one of the chlorine molecules beside the amino terminal groups with a weight loss of 10.069%. The third step occurs within the temperature range of 284-381 °C at DTG_{max} = 328 °C (endo) which was assigned to the loss of organic moiety of *Gln* chelate with a weight loss of 54.740%. The fourth step occurs within the temperature range of 432-800 °C at DTG_{max} = 500 °C which was assigned to the loss of organic moiety with a weight loss of 8.102%. The few carbon atoms with mass (24.906%) in the final product remain stable till 800 °C.

Met-Se complex: The thermal decomposition of *Met*-Se complex (**IV**) occurs in three steps. The first degradation step takes place in the temperature range of 128-146 °C at DTG_{max} = 134 °C (endo) and it corresponds to the loss of chlorine atoms with a weight loss of 11.363%. The second step occurs within the temperature range of 257-303 °C at DTG_{max} = 277 °C (endo) that was assigned to the loss of organic moiety with a weight loss of 56.139%. The third step occurs within the temperature range of 494-535 °C at DTG_{max} = 511 °C that was assigned to the loss of organic moiety with a weight loss of 10.147%. The residual carbon with a mass of 2 2.351% in the final product remains stable till 800 °C.

Cys-Se complex: The thermal decomposition of *Cys*-Se complex (**V**) occurs in three successive steps. The first degradation step takes place in the temperature range of 265-305 °C at DTG_{max} = 284 °C and it corresponds to the loss of two chlorine atoms and two molecules of *Cys* with weight loss of 70.559%. The second step occurs within the temperature range of 381-436 °C at DTG_{max} = 397 °C which was assigned to the loss of organic moiety with a weight loss of 12.665%. The third step occurs within the temperature range of 448-558 °C at DTG_{max} = 509 °C (endo) which was assigned to the loss of organic moiety with a weight loss of 11.700%. The residual few carbon atoms with m(VO_2 + C) in the final product remain stable till 800 °C as a final residue.

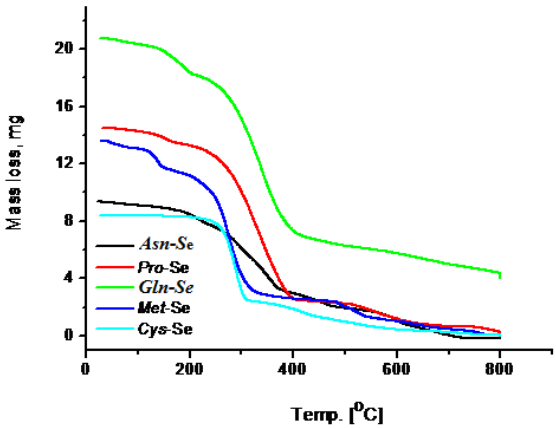

Fig. 13. TG curves of $[Se(AA)_2Cl_2]$ complexes (AA= *Asn*, *Pro*, *Gln*, *Met* and *Cys*).

Antioxidant activity

Bioavailability of selenium from dietary supplements is strongly dependent on its chemical form. Seleno amino acids which possess organically bound selenium are considered to be better absorbed and less toxic than inorganic selenium compounds [37]. Many chemical materials have been evaluated for antioxidant activities using *in vivo* and *in vitro* models and the selenium compounds trial is one of the most successful. The aim of this work was to examine the antioxidant activities of five selenium amino acid complexes. DPPH and hydroxyl radical scavenging methods were applied to *in vitro* models. Resulted data indicated that the radical scavenging activities of the tested compounds depend on the chemical form of selenium. Radical scavenging activity effects of selenium complexes **I-V** against DPPH and hydroxyl radicals are shown

in Figs. 14 and 15. All concentrations (10, 20 and 30 ppm) of the tested complexes showed significant to moderate radical scavenging activity compared to standard BHA material (70.4, 85.1 and 94.3%), respectively. As shown in Figs. 14 and 15, the radical scavenging activity of all tested compounds gradually increases through all concentrations (10, 20 and 30 ppm) compared with butylated hydroxyanisole (BHA) as positive control.

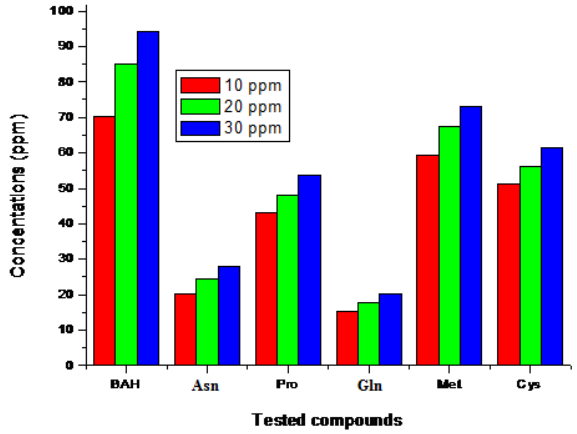

Fig. 14. Diagrams of radical scavenging activity effects of selenium complexes **I-V** against DPPH.

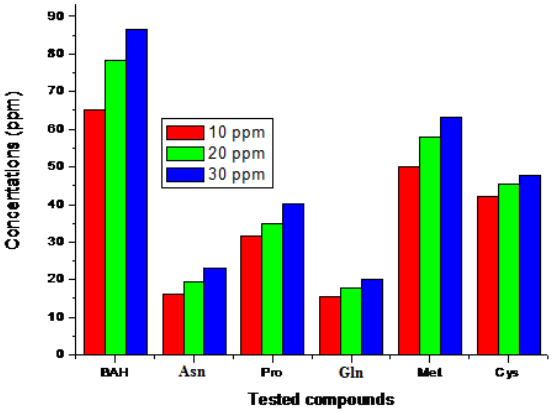

Fig. 15. Diagrams of radical scavenging activity effects of selenium complexes **I-V** against hydroxyl radicals

The Se-*Met* and Se-*Cys* displayed the highest radical scavenging activity effects against DPPH compared with BHA. In the DPPH free radical scavenging test the stable yellow-colored diphenylpicrylhydrazine (DPPH-H) is formed in the presence of an antioxidant. The scavenging effects of BHA at concentrations 10, 20 and 30 ppm on the hydroxyl radical were 65.2, 78.3 and 86.5%, respectively. When the tested compounds or BHA were incubated with the reaction mixture they were able to interfere with free radical reaction and could prevent damage to the sugar.

CONCLUSION

Selenium(IV)-amino acids complexes of *Asn*, *Pro*, *Gln*, *Met*, and *Cys* were synthesized and characterized using analytical techniques such as elemental analysis, thermal analyses and (FT–IR, Raman laser, ^{1}H-NMR, and UV–Vis) spectroscopy. The microanalytical elemental data deduced a 1:2 selenium ions: amino acid ratio of the synthesized complexes. In view of the FT-IR spectroscopy results the selenium (IV) ion was coordinated to the respective amino acids as a bidentate chelate. The geometry of the selenium ions was six-coordinated with those of amino acid complexes. The selenium in nano-structured form was investigated by Raman laser spectroscopy, X-ray powder diffraction, surface morphology, scanning electron microscopy (SEM). The free radical scavenging activity of the newly synthesized selenium (IV) complexes was determined at the concentration of 10, 20 and 30 ppm using stable DPPH free radicals. All complexes displayed a significant antioxidant activity.

Acknowledgements*: This work was funded by the Deanship of Scientific Research at Princess Nourah bint Abdulrahman University, through the Research Groups Program Grant no. (RGP-1438-0003).*

Author Contributions: *Ahmed Naglah, R.F. Hassan and Moamen Refat designed and observed the proposal, contributed to data analysis and interpretation. Wael Hozzien did the biological study and wrote the biological part. Asma S. Al-Wasidi, Nawal M. Al-Jafshar and Jamelah S. Al-Otifi, surveyed data in the database and did the spectral analysis. Ahmed Naglah and Moamen Refat gave conceptual advice and wrote the paper. All authors discussed the results and implications and commented on the manuscript at all stages.*

Conflict of Interests: *The authors declare no conflict of interests.*

REFERENCES

1. Q. Wang, A. R. Parrish, L. Wang. Expanding the genetic code for biological studies, *Chem. Biol*. **16** (3), 323 (2009).
2. P. Newsholme, L. Stenson, M. Sulvucci, R. Sumayao, M. Krause. Amino Acid Metabolism. Comprehensive Biotechnology (2nd ed.), **1**, 3 (2011).
3. K. Asemave, S. G. Yiase, S. O. Adejo, B. A. Anhwange, *International Journal of Inorganic and Bioinorganic Chemistry*, **2** (1), 11 (2011).
4. R. H. Garret, C. M. Grisham, Biochemistry, Sanders, New York, 1995, p. 216.
5. J. H. Ottawa, D. K. Apps, Biochemistry, ELBS, London, 1984.

6. N. Visfiliumurthy, P. Lingaiah, *Ind. J. Chem.* (A), **25,** 875 (1986).
7. T. R. Rap, M. Sahay, R. C. Aggarwal, *St. J. Chem. (A)*, **23**, 214 (1984).
8. A. Marcu, A. Stanilaa, O. Cozar, L. David; *Journal of Optoelectronics and Advanced Materials*, **10**(4), 830 (2008).
9. L. R. Dinelli, T. M. Bezerra, J. J. Sene, *Curr. Res. Chem*., **2**, 18 (2010).
10. S. S. Dara, A Textbook of Environmental Chemistry and Pollution Control, S. Chand and Company Ltd, India, 2005, p. 67.
11. B. H. Xu, K.Y. Huang, Chemistry, Biochemistry of Selenium and its Application in Life Science, Hua East University of Science & Technology Press (Ch). 1994.
12. X. Y. Gao, J. S. Zhang, L. D. Zhang, M. X. Zhu, *China Public Health*, **16**, 421 (2000).
13. B. Gates, B. Mayers, B. Cattle, Y. N. Xia, *Adv. Funct. Mater.*, **12**, 219 (2002).
14. V. V. Kopeikin, S.V. Valueva, A. I. Kipper, L. N. Borovikova, A. P. Filippov, *Polymer Science*, Series A, **45** (4), 374 (2003).
15. X. Y. Gao, J. S. Zhang, L. D. Zhang, *Adv. Mater*., **14**, 290 (2002).
16. X. Zhang, Y. Xie, F. Xu, X. H. Liu, Chin. *J. Inorg. Chem*., **19**, 77 (2003).
17. B. Gates, B. Mayers, A. Grossman, Y. N. Xia, *Adv. Mater*., **14**, 1749 (2002).
18. E. R. dos Santos, R. S. Corrêa, L. V. Pozzi, A. E. Graminha, H. S. Selistre-de-Araújo, F. R. Pavan, A. A. Batista, *Inorg. Chim. Acta*, **463**, 1, (2017).
19. M. Taha, I. Khan, J. A. P. Coutinho, *Journal of Inorganic Biochemistry*, **157**, 25 (2016).
20. S. Choksakulporn, A. Punkvang, Y. Sritana-anant, *Journal of Molecular Structure*, **1082**, 97 (2015).
21. S. Ghasemi, A. H. Khoshgoftarmanesh, M. Afyuni, H. Hadadzadeh, R. Schulin, *Soil Biology and Biochemistry*, **63**, 73 (2013).
22. P. Ramakrishnan, S. Shanmugam, *Journal of Power Sources*, **316**, 60 (2016).
23. W. Brand-Williams, M. E. Cuvelier, C. Berset, Use of a free radical method to evaluate antioxidant activity, *LWT Food Sci. Technol*., **28**, 25 (1995).
24. H. Ohkawa, N. Ohishi, K. Yagi, Assay for lipid peroxides in animal tissues by thiobarbituric acid reaction, *Anal. Biochem*., **95**, 351 (1979).
25. K. Shimoda, K. Fujikawa, K. Yahara, T. Nakamura, Antioxidative properties of xanthan on the autoxidation of soybean oil in cyclodextrin emulsion, *J. Agric. Food Chem*., **40**, 945 (1992).
26. W. J. Geary, *Coord. Chem. Rev*., **7,** 81 (1971).
27. M. S. Refat, *J. Mol. Struct*., **842** (1–3), 24 (2007).
28. C. H. Ramamurthy, K. S. Sampath, P. Arunkumar, M. S. Kumar, V. Sujatha, K. Premkumar, C. Thirunavukkarasu, *Bioprocess and Biosystems Engineering*, **36,** 1131 (2013).
29. E.J. Baran, I. Viera, M.H. Torre, *Spectrochim. Acta*, **66A,** 114 (2007).
30. T.J. Lane, J.A. Durkin, R.J. Hooper, *Spectrochim. Acta*, **20,** 1013 (1964).
31. J.F. Jackovitz, J.L.Walter, *Spectrochim. Acta*, **22,** 1393 (1966).
32. B. Smith, Infrared Spectral Interpretation, CRC Press, Boca Raton, 1999.
33. K. Nakamoto, Infrared and Raman Spectra of Inorganic and Coordination Compounds: Part B, 5th ed., Wiley, New York, 1997.
34. G.B. Deacon, R.J. Phillips, *Coord. Chem. Rev*., **33**, 227(1980).
35. M.S. Refat and Kh. M. Elsabawy, *Bulletin of Material Sciences*, **34**(4), 873 (2011).
36. B.D. Cullity, Elements of X-ray Diffraction, Addison-Wesley Publication Company, Massachusetts, 1978.
37. M. P Rayman, The importance of selenium to human health, *The Lancet*, **356,** 233 (2000).

СИНТЕЗ, ОХАРАКТЕРИЗИРАНЕ И АНТИОКСИДАНТНА АКТИВНОСТ НА КОМПЛЕКСИ НА СЕЛЕН (IV) С НЯКОИ АМИНОКИСЕЛИНИ – БИНУКЛЕАРНИ КОМПЛЕКСИ

А. М. Наглах[1,2*], А. С. Ал-Васиди[3], Н. М. Ал-Джафшар[3], Дж. С. Ал-Отифи[3], М. С. Рефат[4, 5], У. Н. Хоцеин[6, 7]

[1] *Департамент по фармацевтична химия, Катедра по разработване и изследване на лекарства, Колеж по фармация, Университет „Крал Сауд“, Рияд 11451, Саудитска Арабия*

[2] *Департамент по химия на пептидите, Отдел по изследване на химическата индустрия, Национален изследователски център, 12622 Доки, Кайро, Египет*

[3] *Департамент по химия, Научен колеж, Университет „Принцеса Нура Бинт Абдулрахман“, Рияд 11671, Саудитска Арабия*

[4] *Департамент по химия, Научен факултет, Таифски университет, п.к. 888, Ал-Хауиа, Таиф 21974, Саудитска Арабия*

[5] *Департамент по химия, Научен факултет, Университет на Порт Саид, Порт Саид, Египет*

[6] *Катедра по изследване на биопродукти, Департамент по зоология, Научен колеж, Университет „Крал Сауд“, Рияд 11451, Саудитска Арабия*

[7] *Департамент по ботаника и микробиология, Научен факултет, Университет на Бени-Суеф, Бени Суеф 62111, Египет*

Постъпила на 9 януари, 2018 г.; приета на 17 май, 2018 г.

(Резюме)

Получени са комплексите на селен (IV) с аминокиселините аспарагин (*Asn*), пролин (*Pro*), глутамин (*Gln*), метионин (*Met*) и цистеин (*Cys*) и са охарактеризирани чрез елементен анализ, измерване на молната проводимост, спектрални изследвания (IR, Раман, UV-Vis, ^{1}H-NMR и мас-) и термогравиметричен анализ (TG/DTG). Изследванията на рентгеновата дифракция са проведени на дифрактометър PANalytical, повърхностната хомогенност на пробите е изследвана със сканиращ електронен микроскоп Quanta FEG 250 (SEM), а химичният състав на пробите е определен чрез енергийно-дисперсивен рентгенов анализ. Всички комплекси на селен (IV) **(I-V)** са от вида $[Se^{+4}(AA^{-1})_2Cl_2]$, където AA = (*Asn*, *Pro*, *Gln*, *Met* и *Cys*) се отнасят като монобазични лиганди. Масовите фрагменти на комплекса [Se (*Cys*)$_2$(Cl)$_2$] (**V**) подкрепят твърдението за монобазичност. Предполагаемата геометрия на 1:2 комплексите е октаедрична конфигурация с два хлорни атома и два бидентатни лиганда, заемащи ъгловите места в октаедричните комплекси. В комплексите на селен с *Asn*, *Pro*, *Gln* и *Met*, амино и карбоксилните групи участват в координирането с метала, докато *Cys* се координира посредством сулфхидрилната и карбоксилната група. Активността на новосинтезираните комплекси на селен (IV) за отстраняване на свободни радикали е определена при концентрация от 10, 20 и 30 ppm въз основа на взаимодействието със стабилния свободен радикал 1,1-дифенил-2-пикрилхидразил (DPPH). Всички комплекси проявяват добра антиоксидантна активност.